

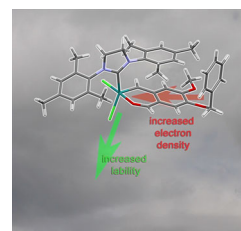
On the chloride lability in electron-rich second-generation ruthenium benzylidene complexes

Simone Strasser¹ · Eva Pump¹ · Roland C. Fischer² · Christian Slugovc¹

Received: 19 March 2015 / Accepted: 23 April 2015
© Springer-Verlag Wien 2015

Abstract A series of electron-rich second-generation *cis*-dichloro ruthenium aldehyde-chelating benzylidene complexes was prepared, characterized, and tested in typical ring-opening metathesis polymerization (ROMP) experiments. The benzylidene precursors were prepared via etherification of the hydroxyl group and vinylation at position 2 of 2-bromo-5-hydroxy-4-methoxybenzaldehyde. The corresponding ruthenium complexes were obtained from a carbene exchange reaction and were characterized by a *cis*-dichloro arrangement. A pronounced lability of the chloride ligand *trans* to the *N*-heterocyclic carbene ligand in methanol was observed and it was shown that this feature is responsible for a particularly slow ROMP in this solvent.

Graphical abstract



Keywords Olefin metathesis · Ruthenium · Structure–activity relationships · Polymerizations

Dedicated to Franz Stelzer and his contributions to the field of Olefin Metathesis.

Electronic supplementary material The online version of this article (doi:10.1007/s00706-015-1484-x) contains supplementary material, which is available to authorized users.

✉ Christian Slugovc
slugovc@tugraz.at

¹ Institute of Chemistry and Technology of Materials, NAWI Graz, Graz University of Technology, Stremayrgasse 9, 8010 Graz, Austria

² Institute of Inorganic Chemistry, NAWI Graz, Graz University of Technology, Stremayrgasse 9, 8010 Graz, Austria

Introduction

Ruthenium-based olefin metathesis catalysts/initiators tolerate a wide array of functional groups including water and to some extent oxygen and are therefore widely used in carbon–carbon double bond forming reactions [1, 2]. Well-defined ruthenium olefin metathesis catalysts/initiators typically feature a square pyramidal coordination geometry generally made up by a carbene as the apex and two neutral ligands such as phosphines or *N*-heterocyclic carbenes (NHCs) as well as two anionic ligands (in most cases chlorides) forming the base. Most prominent, yet most metathetically active examples exhibit a *trans*-dichloro arrangement, but also complexes with a thermodynamic preference for the *cis*-dichloro isomer are known [3, 4]. The latter class is characterized by a slower initiation and a higher thermal stability in comparison to their *trans*-dichloro counterparts which can be rationalized by the widely accepted hypothesis that the *cis*-dichloro species

itself is not metathesis active but has to isomerize to its metathesis active *trans*-dichloro counterpart [5, 6]. The isomerization process occurs in a dissociative or a concerted manner [3]. Second-generation (i.e., bearing an *N*-heterocyclic carbene coligand) *cis*-dichloro ruthenium benzylidenes with, e.g., oxygen- [7–9], vinyl- [10], sulfur- [11], or nitrogen-based [12, 13] neutral coligands are known. A comprehensive overview including calculated relative thermodynamic stabilities of the *cis*- and the *trans*-isomers has been published recently [3]. The combination of slow initiation and thermal stability makes *cis*-dichloro pre-catalysts/initiators interesting for olefin metathesis reactions in which slow dosing at elevated temperatures is desired [14–18] or when a thermally triggered polymerization is intended [8, 12, 13].

Herein we report on our investigations to increase the electron density of the oxygen chelated benzylidene ligand used in previously disclosed (SPY-5-31) dichloro(2-formylbenzylidene- κ^2 (C,O))(1,3-bis(2,4,6-trimethylphenyl)-4,5-dihydroimidazol-2-ylidene)ruthenium (**5**) [8]. The study was conducted following two goals; first, the parent compound **5** is not particularly soluble in nonpolar solvents and upon introduction of long alkyl chains an increase of solubility can be expected. Second, as it is known that the initiation efficacy can be reduced by increasing the electron density in related ester chelated benzylidene complexes [19], a further reduction of the initiation efficacy of **5** might be feasible [8].

Results and discussion

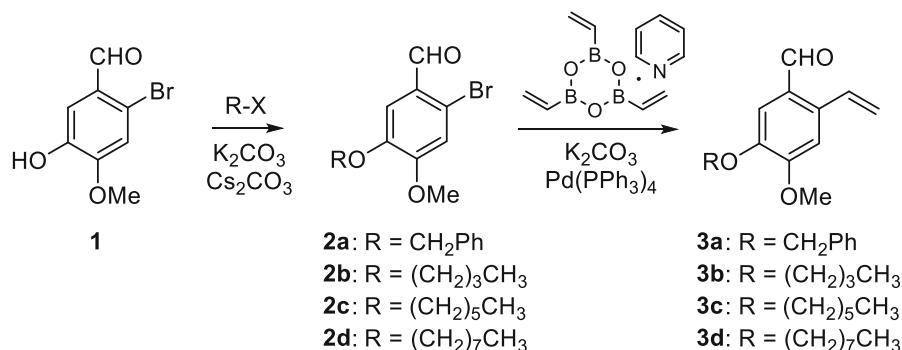
Aiming at the preparation of aldehyde-chelating benzylidene complexes with different solubility in apolar media, a series of differently substituted 2-vinyl-5-alkoxy-4-methoxybenzaldehyde derivatives was envisaged. Carbene precursors should feature a benzyloxy (**3a**), an *n*-butyloxy (**3b**), an *n*-hexyloxy (**3c**), or an *n*-octyloxy group (**3d**) in

position 5 (see Scheme 1). Carbene precursors **3a–3d** were prepared in a two-step procedure starting from commercially available 2-bromo-5-hydroxy-4-methoxybenzaldehyde (**1**). In the first step, etherification of the phenolic hydroxyl group using the corresponding alkyl bromides or iodides was carried out following a slightly modified procedure [20]. Instead of acetone, dimethylformamide was used as the solvent and additionally to K_2CO_3 , 2.5 mol % Cs_2CO_3 (in respect of K_2CO_3) were added to the reaction mixture. The reactions were performed at room temperature for 24 h. Compounds **2a–2d** were obtained in 80–83 % yield after chromatographic purification.

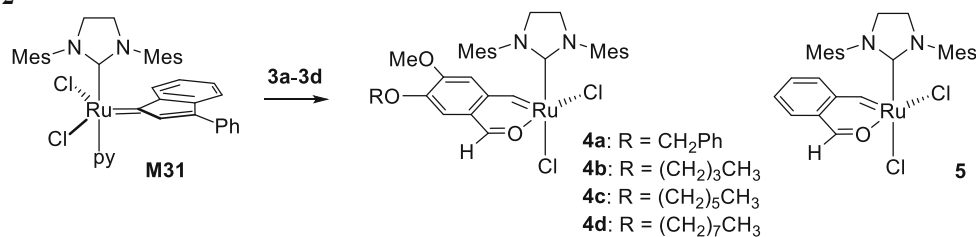
In the second step, a Suzuki–Miyaura cross-coupling using 2,4,6-trivinylcyclotriboroxane anhydride pyridine complex as the coupling partner, 3 mol % $Pd(PPh_3)_4$ as the catalyst, and K_2CO_3 as the base was carried out. Compounds **3a–3d** were obtained in 77–96 % yield upon column chromatographic purification. The desired ruthenium benzylidene derivatives **4a–4d** were then prepared by stirring a solution of 1 equiv. **M31** and 1.15 equiv. **3a–3d** in dichloromethane at room temperature for several hours, whereupon the color of the solution turned from wine-red to deep green (see Scheme 2). Extraction of the reaction mixture with aqueous HCl was carried out to remove pyridine from the reaction mixture to avoid the occurrence of some pyridine coordinated impurities [19]. Complexes **4a–4d** were then obtained upon column chromatographic purification, followed by a second extraction procedure with aqueous HCl in 53–73 % yield. The second extraction was necessary to remove an unknown second carbene-bearing complex which emerged during the chromatographic purification (vide infra).

The complexes were characterized by 1H and ^{13}C NMR spectroscopy, elemental analysis, and an exemplary single crystal X-ray crystallographic structure determination of **4a**. 1H NMR spectroscopy in $CDCl_3$ as the solvent immediately suggested *cis*-dichloro structures in all cases. Distinct signals for all 4 aromatic mesityl protons and all 6

Scheme 1



Scheme 2



mesityl methyl groups as well as a diastereotopic splitting of the methylene group attached to the oxygen in position 5 were observed indicating a chiral ruthenium center as it is present in *cis*-dichloro configured complexes of this type [4, 8, 9, 12]. Characteristic ¹H NMR signals comprised the carbene's proton at 18.59 ppm in case of **4a** and 18.43–18.44 ppm in case of **4b–4d**, the aldehyde's protons at 9.59 ppm in case of **4a** and 9.72–9.73 ppm in case of **4b–4d**. Characteristic signals in the ¹³C{¹H} NMR spectra were observed at 283.7 ppm (**4a**) and 284.1 ppm (**4b–4d**) and assigned to the carbene carbon. The aldehyde carbons of all four complexes gave resonance at 213.95 ± 0.5 ppm and all NHC-carbene carbons were observed at 204.15 ± 0.5 ppm. These data suggest that the substitution at the oxygen in position 5 has only minor consequences for the electronic properties of the atoms coordinated to the ruthenium center. Furthermore, data make evident, that the electron density in these derivatives is increased compared to the not alkoxyated parent derivative **5** [8]. In **5**, the ¹H NMR shifts for the carbene and the aldehyde are 18.86 and 10.03 ppm, the ¹³C{¹H} NMR shifts for the carbene, the aldehyde, and the NHC are 285.8, 213.4, and 206.4 ppm. The suggested solution structure was also found in the solid state when determining the single crystal X-ray structure of crystals of complex **4a** grown upon slow evaporation of CH₂Cl₂ solution of **4a**. Compound **4a** co-crystallizes with 1 equiv. of CH₂Cl₂ in the centrosymmetric space group *P* $\bar{1}$ and displays a distorted square pyramidal coordination geometry of the ruthenium central atom with the two chlorides in *cis* arrangement, the carbonyl oxygen O(1), and the C(1) atom of the H₂IMes ligand forming the base. The apex is formed by the carbene carbon atom C(1). The Ru–Cl bonds differ ca. 0.022 Å in the solid state, with the longer Cl(1)–Ru(1) distance found for the chlorine atom *trans* to the NHC-ligand. Important structural features of **4a** are listed in Table 1 and set into comparison with the according values from the parent complex **5** [21]. Noticeable are the higher bonding distances around ruthenium in **4a** when compared to **5**, which are a consequence of the higher electron density in **4a** (Fig. 1).

In a next step, the solubility of complexes **4a–4d** and **5** was investigated. As can be seen in Table 2, the solubility

Table 1 Important bond lengths/Å of complexes **4a** and **5** [21]

	4a	5
Ru–C(1)	2.013(1)	2.004(2)
Ru–C(22)	1.830(1)	1.827(2)
Ru–O(1)	2.0583(9)	2.0487(16)
Ru–Cl(1)	2.3877(3)	2.3600(6)
Ru–Cl(2)	2.3654(3)	2.3548(6)

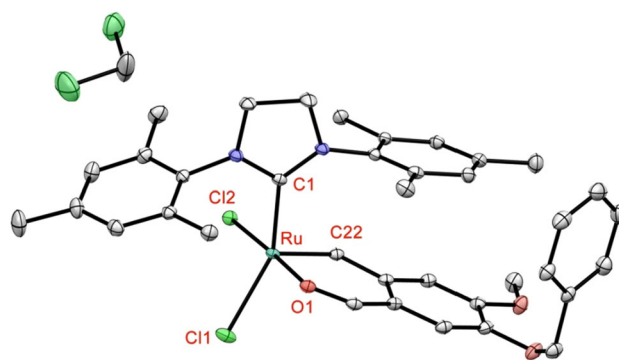


Fig. 1 ORTEP plot of **4a** CH₂Cl₂ (displacement ellipsoids at 50 % probability level, hydrogen omitted for clarity)

of **4a** and **5** in aprotic solvents is generally worse than the solubility of **4b–4d**. As expected, **4d** exhibits the best solubility in nonpolar media and its good solubility in dicyclopentadiene (DCPD) makes this compound a potentially attractive initiator for the bulk-polymerization of this monomer (*vide infra*). All derivatives show an appealing solubility in methanol, which is surprising due to the fact that methanol is often used as non-solvent in purification procedures of similar complexes [18, 22].

Initiators **4a–4d** and **5** were tested in the polymerization of monomer **6** (see Fig. 2) by following the reaction via ¹H NMR spectroscopy at room temperature. The polymerization was generally slow and polymerization half-lives were determined to be 1 days 18 ± 1 h for initiators **4b–4d**, 2 days 12 ± 1 h for initiator **5**, and 7 days 6 ± 3 h for initiator **4a**. Because the propagating species is the same in all cases, the different polymerization speeds can be

Table 2 Solubility of complexes **4a–4d** and **5** determined at 25 °C (low means $<0.1 \text{ mg cm}^{-3}$, fair means $0.1\text{--}0.5 \text{ mg cm}^{-3}$, good means $0.5\text{--}1 \text{ mg cm}^{-3}$, high means $>1 \text{ mg cm}^{-3}$)

	4a	4b	4c	4d	5
Cyclohexane	Low	Low	Low	Fair	Low
Dicyclopentadiene ^a	Low	Fair	Fair	Good	Fair
Et ₂ O	Low	Low	Low	Fair	Low
CH ₂ Cl ₂	Fair	High	High	High	Good
MeOH	Good	High	High	High	High

^a Determined at 33 °C

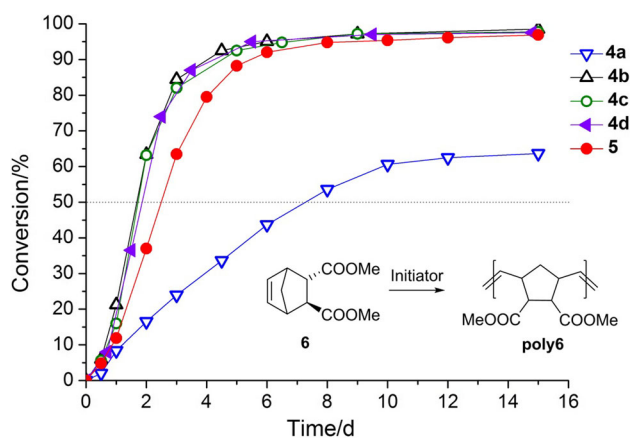


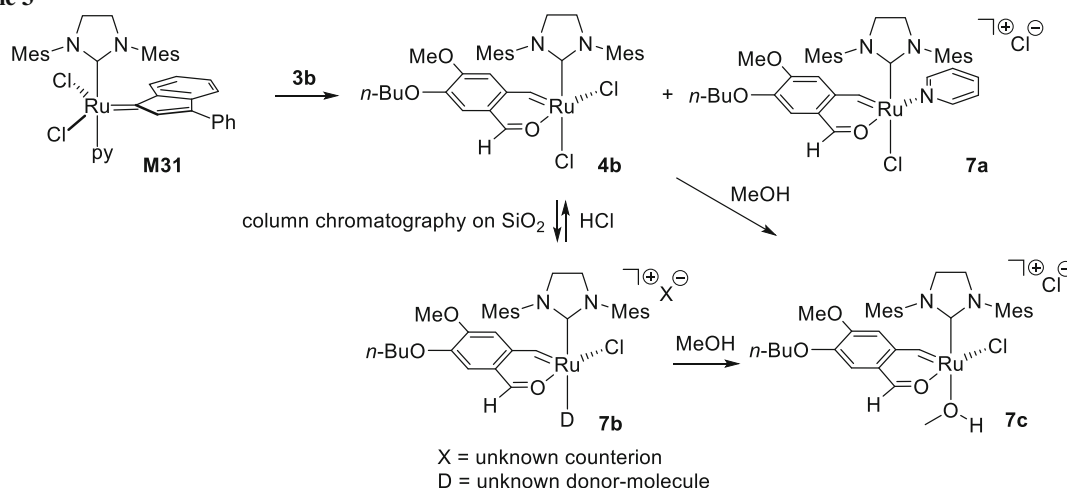
Fig. 2 Time conversion plot of the polymerization of monomer **6** with initiators **4a–4d** and **5** in CDCl_3 at 20 °C under inert atmosphere of N_2 ; $c_{\text{Monomer}} = 0.06 \text{ mol dm}^{-3}$; $[\text{Monomer}]:[\text{Initiator}] = 10:1$; exp. data shown as symbols; solid lines visual aids

deduced to a different initiation efficacy under the chosen reaction conditions. The electron-rich derivatives **4b–4d** exhibited a higher initiation efficacy than the parent

compound **5**. This finding is in strong contrast to the results obtained for similar ester-chelating complexes. In these cases, electron-rich derivatives exhibited a lower initiation efficacy [19]. The slow polymerization with **4a** is readily explained by the poor solubility of **4a** in CDCl_3 which is similar to the solubility in CH_2Cl_2 .

A similar trend for the initiation efficacy can be gained when polymerizing 300 equiv. monomer **6** with 1 equiv. of initiators under investigation in refluxing CH_2Cl_2 ($c_{\text{Monomer}} = 1 \text{ mol dm}^{-3}$). Reaction time was 48 h and monomer **6** was completely consumed after that time in all cases. The number-average molecular mass (M_n) of the resulting polymers, determined via size exclusion chromatography in THF relative to poly(styrene) standards, is $710,000 \text{ g mol}^{-1}$ in case of initiator **5** and in the range of $600,000\text{--}750,000 \text{ g mol}^{-1}$ when using initiators **4a–4d**. The polydispersity index (PDI) was in all cases 2.0 ± 0.2 . For comparison, full initiation would release **poly6** characterized by a M_n of $45,000 \text{ g mol}^{-1}$ and a PDI of 1.07 [23]. Switching to toluene as the solvent and polymerizing at 80 °C no significant differences in the M_n values for polymers prepared with all five initiators could be retrieved ($M_n = 86,000 \pm 6000 \text{ g mol}^{-1}$; PDI = 2.3 ± 0.2). Polymerizations were completed in less than 2 h under these conditions. Further, initiators were tested in the polymerization of neat DCPD. For this purpose, the polymerization was monitored by simultaneous thermal analysis (STA) [24]. An initiator loading of 40 ppm was investigated maintaining a heating rate of 3 °C min^{-1} . Under these conditions the heat evolution of the polymerization peaked at $90 \pm 5 \text{ °C}$ in case of initiators **4a–4d** and $70 \pm 5 \text{ °C}$ in case of **5**. Due to the concurring thermally induced retro-Diels–Alder reaction of DCPD [24], a mass loss occurred which amounts to $25 \pm 5 \%$ for tries initiated

Scheme 3



with **4a–4d** and to 10 ± 2 % when **5** is used as the initiator. Both results lead to the conclusion that the initiation efficacy of the complexes is switched under these conditions, i.e., **5** initiates faster than **4a–4d**. The improved solubility of **4d** in DCPD did not translate into a better performance under the studied conditions. Accordingly, the initiators solubility in DCPD seems to be uncritical under the tested conditions (generally, the solubility of the initiators in DCPD is an important factor for the performance of the polymerization; see [25]).

Having established a principal activity profile of the new initiators, we focused our attention on the carbene-bearing by-products which were formed during the synthesis of **4a–4d**. Exemplified by a closer discussion of the synthesis of **4b**, two side-products were observed. In the crude reaction mixture two carbene-bearing complexes (approx. in 8:2 ratio) were present, which can be separated by column chromatography. The main product was identified to be **4b**, while the identity of the by-product could not be fully established. However, NMR data suggest the coordination of a pyridine to the ruthenium center and a carbene-proton shift of 17.91 ppm (CDCl_3) was observed. In analogy to prior work [19, 26], the compound is tentatively identified as the cationic species **7a**. A full characterization and especially tries to crystallize **7a** failed. A second carbene-bearing by-product, not present in the crude reaction mixture, was observed after column chromatography when sampling the fraction containing **4b**. This by-product occurred in approx. 10 mol% and is characterized by a resonance for the carbene-proton at 19.16 ppm and can be easily removed by extracting a CH_2Cl_2 solution of a mixture of **4b** and **7b** with aqueous HCl.

Therefore, we assume that during chromatography the most labile halogen [27] is exchanged for another (unknown) anion which either coordinates to the ruthenium center or, more likely, is dissociated and the fifth coordination site of ruthenium is coordinated by a donor molecule, e.g., methanol. To substantiate this hypothesis, we dissolved purified and unpurified **4b** (containing the unknown impurity **7b**) in methanol- d_4 and recorded NMR spectra of both solutions. The corresponding ^1H NMR spectra were identical, showing a single carbene-resonance

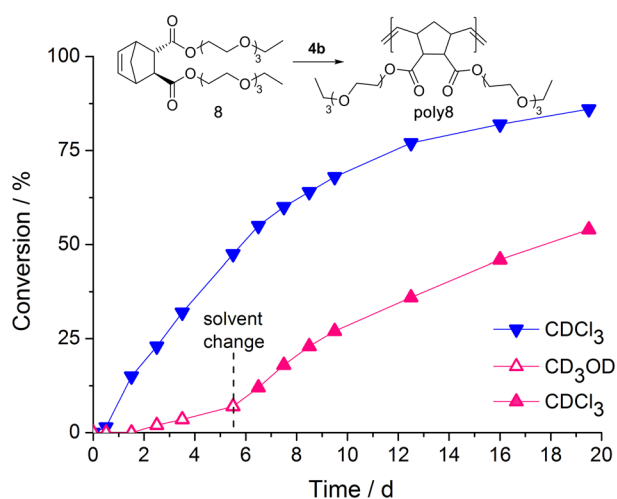
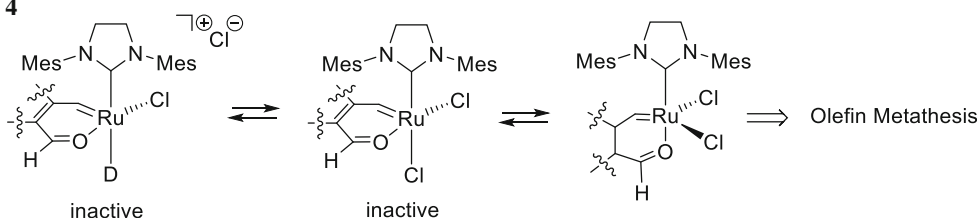


Fig. 3 Time conversion plot of the polymerization of monomer **8** with initiator **4b** in CDCl_3 and in methanol- d_4 at 20 °C under inert atmosphere of N_2 ; $c_{\text{Monomer}} = 0.13 \text{ mol dm}^{-3}$, [Monomer]:[Initiator] = 70:1; exp. data shown as symbols; solid lines visual aids

at 19.11 ppm. Diastereotopic splitting of the O- CH_2 group, but also of the mesityl signals, were indicative for a chiral Ru-center consistent with the proposed structure **7c** (see Scheme 3). Removal of methanol- d_4 , drying in vacuum and acquisition of NMR spectra in CDCl_3 allowed for observing the same product mixture as present in unpurified **4b**, indicating the reversibility of the process. Performing the above described benchmark polymerization of monomer **6** with unpurified **4b** in the NMR tube led to a similar time-conversion profile for the polymerization. Additionally, the carbene region was monitored and a slow vanishing of the carbene signal at 19.16 ppm in favor of the formation of a novel aldehyde signal at 10.57 ppm was found, suggesting that the cationic species **7b** is sensitive towards residual oxygen in the solution. To address the question if **4b** or **7b** is the actual initiator, the course of the polymerization of the methanol and chloroform-soluble monomer **8** (resulting in the chloroform and methanol soluble **poly8**) [28] was studied via NMR spectroscopy in both solvents. Results are depicted in Fig. 3. The polymerization of **8** in CDCl_3 at room temperature was slow

Scheme 4



(half-life: approx. 6 days) and reached a conversion of 85 % after 19 days. In contrast, the polymerization in methanol- d_4 was even slower and only 7 % conversion of **8** was found after 5 days and 12 h. After that time, methanol- d_4 was removed and the residue was dissolved in CDCl_3 , leading to an acceleration of the further course of the reaction.

The observed solvent effect can be either explained by a competition of methanol- d_4 with the monomer for the vacant coordination site or, more likely, with the inactivity of the cationic species **7c** in olefin metathesis. As it is known, that the actual active initiator is a *trans*-dichloro derivative which is in equilibrium with its *cis*-dichloro isomer. The latter features a pronounced lability of the chloride ligand *trans* to the NHC-ligand [29] leading to the observed cationic species in polar medium. Accordingly, a concurring reaction pathway is operating which shifts the equilibrium apart from the formation of the *trans*-dichloro derivative (see Scheme 4). The lability of the chloride ligand and the corresponding pre-equilibrium might also be the reason for solvent effects previously observed in olefin metathesis [30].

In conclusion, we disclosed a family of electron-rich aldehyde-chelating *cis*-dichloro configured benzylidene complexes. Their electron-richness results in a pronounced lability of the chloride in *trans*-position to the *N*-heterocyclic carbene ligand. The resulting cationic complexes exhibit a good solubility in the polar protic solvent methanol. The formation of such cationic species is detrimental for catalyzing (or initiating) olefin metathesis reactions as their existence lowers the relative concentration of the actual active pre-catalyst (or initiator) in solution. The findings disclosed here might be of general significance for any ruthenium-mediated olefin metathesis transformation and constitute a further building-block for explaining hitherto ununderstood solvent effects.

Experimental

Umicore **M31** was received from Umicore AG [23]. 2-Bromo-5-hydroxy-4-methoxybenzaldehyde (**1**), 2,4,6-trivinylcyclotriboroxane-pyridine complex, and $\text{Pd}(\text{PPh}_3)_4$, were purchased from Aldrich and were used as received. *endo,exo*-Bicyclo[2.2.1]hept-5-ene-2,3-dicarboxylic acid dimethyl ester (**6**) [31], *endo,exo*-bicyclo[2.2.1]hept-5-ene-2,3-dicarboxylic acid bis[2-[2-(2-ethoxyethoxy)ethoxy]ethyl] ester (**8**) [28], and (*SPY-5-31*)-dichloro(2-formylbenzylidene- $\kappa^2(\text{C},\text{O})$)(1,3-bis(2,4,6-trimethylphenyl)-4,5-dihydroimidazol-2-ylidene)ruthenium (**5**) [8] were prepared according to literature methods. Elemental analyses (C, H, N) were conducted on an Elementar vario EL machine, and results were found to be in agreement (± 0.3 %) with the calculated values. The number-average

molecular weights (M_n) and polydispersity indices (PDI) were determined by size exclusion chromatography (SEC) using THF as solvent in the following arrangement: Merck Hitachi L6000 pump, separation columns of Polymer Standards Service, 8×300 mm STV $5 \mu\text{m}$ grade size (10^6 , 10^4 , and 10^3 Å), refractive index detector from Wyatt Technology, model Optilab DSP interferometric refractometer. Polystyrene Standards purchased from Polymer Standard Service were used for calibration. NMR spectra were recorded on Bruker Avance 300 MHz or Varian INOVA 500 MHz spectrometers. STA measurements were performed with a Netzsch Simultaneous Thermal Analyzer STA 449C (crucibles: aluminum from Netzsch) and was operated with a helium flow rate of $50 \text{ cm}^3 \text{ min}^{-1}$ used in combination with a protective gas flow of $8 \text{ cm}^3 \text{ min}^{-1}$.

(*SPY-5-31*) Dichloro(4-benzyloxy-2-formyl-5-methoxybenzylidene- $\kappa^2(\text{C},\text{O})$)(1,3-bis(2,4,6-trimethylphenyl)-4,5-dihydroimidazol-2-ylidene)ruthenium

(**4a**, $\text{C}_{37}\text{H}_{40}\text{Cl}_2\text{N}_2\text{O}_3\text{Ru}$)

Complex **M31** (373.9 mg, 0.50 mmol) was dissolved in 5 cm^3 dry degassed CH_2Cl_2 in a Schlenk flask and 161.0 mg **3a** (0.60 mmol) dissolved in 2 cm^3 CH_2Cl_2 was added under inert atmosphere of nitrogen. The reaction mixture was stirred at room temperature for 4 h, whereupon its color turned from deep red to deep green. The reaction mixture was transferred into a separation funnel and two times extracted with 5 cm^3 HCl (0.5 M) and subsequently with 5 cm^3 H_2O . The organic phase was collected, dried over Na_2SO_4 , and the volume of the solvent was reduced to about 1 cm^3 . Upon precipitation with *n*-pentane a green powder formed, which was collected on a glass frit and dried in vacuo. Subsequent purification by column chromatography (SiO_2 , CH_2Cl_2 and $\text{CH}_2\text{Cl}_2/\text{MeOH}$, 20:1–10:1, (v:v)) and sampling the spot at $R_f = 0.62$ [$\text{CH}_2\text{Cl}_2/\text{MeOH}$, 10:1, (v:v)] gave the crude product. This product was redissolved in 5 cm^3 CH_2Cl_2 and two times extracted with 5 cm^3 HCl (0.5 M) and subsequently with 5 cm^3 H_2O . Removal of the solvent and drying in vacuum gave pure **4a**. Yield: 213.2 mg (62 %) green microcrystals; ^1H NMR (300 MHz, CDCl_3): $\delta = 18.59$ (s, 1H, Ru = CH), 9.59 (s, 1H, CHO), 7.52 (s, 1H, bz), 7.50 (s, 1H, bz), 7.39–7.24 (m, 3H^{bz}, 1H^{mes}), 7.20 (bs, 1H, mes), 6.95 (s, 1H, ph⁶), 6.82 (bs, 1H, mes), 6.54 (s, 1H, ph³), 5.48 (bs, 1H, mes), 5.15 (m, 1H, CH₂^{bz}), 5.07 (m, 1H, CH₂^{bz}), 4.28–3.43 (m, 4H, Im), 3.95 (s, 3H, OCH₃), 2.70 (s, 3H, CH₃^{mes}), 2.45 (s, 6H, CH₃^{mes}), 2.00 (s, 3H, CH₃^{mes}), 1.58 (s, 3H, CH₃^{mes}), 0.88 (s, 3H, CH₃^{mes}) ppm; $^{13}\text{C}\{^1\text{H}\}$ NMR (75 MHz, CDCl_3): $\delta = 283.7$ (1C, Ru = CH), 213.9 (1C_q, CNN), 204.1 (1C, CHO), 156.8 (1C_q, ph⁵), 147.0 (1C_q, ph⁴), 140.4, 139.9 (2C_q, C^{mes-N}), 138.2, 137.9, 137.8, 135.2, 135.4, 131.6 (6C_q, C^{mes}), 130.9, 130.1, 129.3, 128.4 (4C, mes), 136.0 (1C_q, bz¹), 130.8 (1C_q, ph¹), 128.7, 128.1

(4C, bz^{2,3,5,6}), 128.2 (1C, bz⁴), 121.8 (1C_q, ph²), 120.0 (1C_q, ph³), 108.1 (1C_q, ph⁶), 70.5 (1C, CH₂^{bz}), 56.3 (1C, OCH₃), 53.6, 51.0 (2C, Im), 21.6, 20.7, 20.3, 18.5, 18.4, 16.6 (6C, CH₃^{mes}) ppm.

(SPY-5-31) *Dichloro(4-butyloxy-2-formyl-5-methoxybenzylidene-κ²(C,O))(1,3-bis(2,4,6-trimethylphenyl)-4,5-dihydroimidazol-2-ylidene)ruthenium*

(4b, C₃₄H₄₂Cl₂N₂O₃Ru)

Complex **4b** was synthesized similarly to **4a** using 250.0 mg **M31** (0.33 mmol) and 90.1 mg **3b** (0.38 mmol) as the starting materials. Yield: 151.8 mg (65 %) green crystals; TLC: R_f = 0.45 (SiO₂, CH₂Cl₂/MeOH, 10:1, (v:v)); ¹H NMR (300 MHz, CDCl₃): δ = 18.43 (s, 1H, Ru = CH), 9.72 (s, 1H, CHO), 7.29 (bs, 1H, mes), 7.18 (bs, 1H, mes), 7.00 (s, 1H, ph⁶), 6.90 (bs, 1H, mes), 6.53 (s, 1H, ph³), 5.95 (bs, 1H, mes), 4.33–3.49 (m, 4H, Im), 4.01–3.78 (t, 2H, OCH₂(CH₂)₂CH₃), 3.93 (s, 3H, OCH₃), 2.72 (s, 3H, CH₃^{mes}), 2.50 (s, 3H, CH₃^{mes}), 2.44 (s, 6H, CH₃^{mes}), 2.06 (s, 3H, CH₃^{mes}), 1.80 (m, 2H, OCH₂CH₂CH₂CH₃), 1.52 (m, 2H, O(CH₂)₂CH₂CH₃), 1.05 (s, 3H, CH₃^{mes}), 0.99 (t, 3H, ³J_{HH} = 7.4 Hz, O(CH₂)₃CH₃) ppm; ¹³C{¹H} NMR (75 MHz, CDCl₃): δ = 284.1 (1C, Ru=CH), 213.9 (1C_q, CNN), 204.2 (1C, CHO), 156.5 (1C_q, ph⁵), 148.5 (1C_q, ph⁴), 140.3, 139.9 (2C_q, C^{mes-N}), 138.24, 138.20, 137.8, 135.6, 135.2, 131.6 (6C_q, C^{mes}), 130.9, 130.1, 129.5, 128.4 (4C, mes), 130.8 (1C_q, ph¹), 122.2 (1C_q, ph²), 118.3 (1C_q, ph³), 108.1 (1C_q, ph⁶), 69.4 (1C, OCH₂(CH₂)₂CH₃), 56.3 (1C, OCH₃), 51.04, 50.97 (2C, Im), 31.1 (1C, OCH₂CH₂CH₂CH₃), 21.5, 20.8, 20.2, 18.5, 18.4, 16.8 (6C, CH₃^{mes}), 19.3 (1C, O(CH₂)₂CH₂CH₃), 14.1 (1C, O(CH₂)₃CH₃) ppm; ¹H NMR (300 MHz, CD₃OD): δ = 19.11 (s, 1H, Ru=CH), 9.96 (s, 1H, CHO), 7.66 (s, 1H, ph⁶), 7.14 (s, 2H, mes), 6.96 (s, 1H, ph³), 6.67 (s, 2H, mes), 4.29 (m, 1H, OCH₂(CH₂)₂CH₃), 4.19 (m, 1H, OCH₂(CH₂)₂CH₃), 4.08 (s, 3H, OCH₃), 3.84 (s, 4H, Im), 2.42 (s, 6H, CH₃^{mes}), 2.30 (s, 6H, CH₃^{mes}), 1.94 (s, 6H, CH₃^{mes}), 1.91 (m, 2H, OCH₂CH₂CH₂CH₃), 1.60 (m, 2H, O(CH₂)₂CH₂CH₃), 1.05 (t, 3H, ³J_{HH} = 7.4 Hz, O(CH₂)₃CH₃) ppm.

(SPY-5-31) *Dichloro(2-formyl-4-hexyloxy-5-methoxybenzylidene-κ²(C,O))(1,3-bis(2,4,6-trimethylphenyl)-4,5-dihydroimidazol-2-ylidene)ruthenium*

(4c, C₃₆H₄₆Cl₂N₂O₃Ru)

Complex **4c** was synthesized similarly to **4a** using 250.1 mg **M31** (0.33 mmol) and 100.9 mg **3c** (0.38 mmol) as the starting materials. Yield: 128.2 mg (53 %) green microcrystals; TLC: R_f = 0.55 (SiO₂, CH₂Cl₂/MeOH, 10:1, (v:v)); ¹H NMR (300 MHz, CDCl₃): δ = 18.44 (s, 1H, Ru=CH), 9.72 (s, 1H, CHO), 7.29 (bs, 1H, mes), 7.19 (bs, 1H, mes), 7.01 (s, 1H, ph⁶), 6.91 (bs, 1H, mes), 6.56 (s, 1H, ph³), 5.97 (bs, 1H, mes), 4.31–3.50 (m, 4H, Im), 4.03–3.79 (t, 2H, OCH₂(CH₂)₄CH₃), 3.93 (s, 3H, OCH₃), 2.74 (s, 3H, CH₃^{mes}), 2.52 (s, 3H, CH₃^{mes}), 2.43 (s, 6H, CH₃^{mes}), 2.08 (s,

3H, CH₃^{mes}), 1.83 (m, 2H, OCH₂CH₂(CH₂)₃CH₃), 1.52 (m, 2H, O(CH₂)₂CH₂(CH₂)₂CH₃), 1.37 (m, 4H, O(CH₂)₃(CH₂)₂CH₃), 1.06 (s, 3H, CH₃^{mes}), 0.93 (t, 3H, ³J_{HH} = 6.7 Hz, O(CH₂)₅CH₃) ppm; ¹³C{¹H} NMR (75 MHz, CDCl₃): δ = 284.1 (1C, Ru = CH), 214.0 (1C_q, CNN), 204.1 (1C, CHO), 156.6 (1C_q, ph⁵), 148.6 (1C_q, ph⁴), 140.4, 134.0 (2C_q, C^{mes-N}), 138.4, 138.2, 137.8, 135.2, 135.7, 131.6 (6C_q, C^{mes}), 130.9 (1C_q, ph¹), 130.1, 129.8, 129.6, 128.5 (4C, mes), 122.2 (1C_q, ph²), 118.3 (1C_q, ph³), 108.2 (1C_q, ph⁶), 69.7 (1C, OCH₂(CH₂)₄CH₃), 56.3 (1C, OCH₃), 51.0 (2C, Im), 31.7 (1C, OCH₂CH₂(CH₂)₃CH₃), 29.0 (1C, O(CH₂)₂CH₂(CH₂)₂CH₃), 25.9 (1C, O(CH₂)₃CH₂CH₂CH₃), 22.8 (1C, O(CH₂)₄CH₂CH₃), 21.5, 20.9, 20.3, 18.5, 18.4, 16.8 (6C, CH₃^{mes}), 14.2 (1C, O(CH₂)₅CH₃) ppm.

(SPY-5-31) *Dichloro(2-formyl-5-methoxy-4-octyloxybenzylidene-κ²(C,O))(1,3-bis(2,4,6-trimethylphenyl)-4,5-dihydroimidazol-2-ylidene)ruthenium*

(4d, C₃₈H₅₀Cl₂N₂O₃Ru)

Complex **4d** was synthesized similarly to **4a** using 250.0 mg **M31** (0.33 mmol) and 100.9 mg **3d** (0.38 mmol) as the starting materials. Yield: 185.3 mg (73 %) green microcrystals; TLC: R_f = 0.57 (SiO₂, CH₂Cl₂/MeOH, 10:1, (v:v)); ¹H NMR (300 MHz, CDCl₃): δ = 18.44 (s, 1H, Ru=CH), 9.73 (s, 1H, CHO), 7.29 (bs, 1H, mes), 7.19 (bs, 1H, mes), 7.02 (s, 1H, ph⁶), 6.91 (bs, 1H, mes), 6.56 (s, 1H, ph³), 5.98 (bs, 1H, mes), 4.31–3.49 (m, 4H, Im), 4.05–3.79 (t, 2H, OCH₂(CH₂)₄CH₃), 3.93 (s, 3H, OCH₃), 2.73 (s, 3H, CH₃^{mes}), 2.52 (s, 3H, CH₃^{mes}), 2.43 (s, 6H, CH₃^{mes}), 2.08 (s, 3H, CH₃^{mes}), 1.83 (m, 2H, OCH₂CH₂(-CH₂)₅CH₃), 1.50 (m, 2H, O(CH₂)₂CH₂(CH₂)₄CH₃), 1.42–1.23 (m, 8H, O(CH₂)₃(CH₂)₄CH₃), 1.06 (s, 3H, CH₃^{mes}), 0.90 (t, 3H, ³J_{HH} = 6.6 Hz, O(CH₂)₅CH₃) ppm; ¹³C{¹H} NMR (75 MHz, CDCl₃): δ = 284.1 (1C, Ru = CH), 214.0 (1C_q, CNN), 204.1 (1C, CHO), 156.6 (1C_q, ph⁵), 148.6 (1C_q, ph⁴), 140.4, 139.9 (2C_q, C^{mes-N}), 138.4, 138.2, 137.8, 135.2, 135.7, 131.6 (6C_q, C^{mes}), 131.0 (1C_q, ph¹), 130.1, 129.8, 129.6, 128.5 (4C, mes), 122.2 (1C_q, ph²), 118.3 (1C_q, ph³), 108.2 (1C_q, ph⁶), 69.7 (1C, OCH₂(CH₂)₆CH₃), 56.3 (1C, OCH₃), 51.0 (2C, Im), 32.0 (1C, OCH₂CH₂(-CH₂)₅CH₃), 29.5 (1C, O(CH₂)₂CH₂(CH₂)₄CH₃), 29.4 (1C, O(CH₂)₃CH₂(CH₂)₃CH₃), 29.1 (1C, O(CH₂)₄CH₂(CH₂)₂CH₃), 26.2 (1C, O(CH₂)₅CH₂CH₂CH₃), 22.8 (1C, O(CH₂)₆CH₂CH₃), 21.5, 20.9, 20.3, 18.5, 18.4, 16.8 (6C, CH₃^{mes}), 14.2 (1C, O(CH₂)₇CH₃) ppm.

Chloro(4-butyloxy-2-formyl-5-methoxybenzylidene-κ²(C,O))(pyridine)(1,3-bis(2,4,6-trimethylphenyl)-4,5-dihydroimidazol-2-ylidene)ruthenium chloride

(7a, C₃₉H₄₇Cl₂N₃O₃Ru)

Complex **7a** was obtained during the purification of **4b** via column chromatography sampling the spot at R_f = 0.10 (CH₂Cl₂/MeOH, 10:1, (v:v)). Yield: 38.0 mg (16 %) deep green microcrystals; ¹H NMR (300 MHz, CDCl₃):

$\delta = 17.80$ (s, 1H, Ru=CH), 9.93 (s, 1H, CHO), 8.59 (d, 2H, $^4J_{\text{HH}} = 5.0$ Hz, py^{2,6}), 7.76 (t, 1H, $^3J_{\text{HH}} = 7.0$ Hz, py⁴), 7.60 (s, 1H, ph⁶), 7.47 (s, 1H, ph³), 7.33 (dd, 2H, $^3J_{\text{HH}} = 5.9$ Hz, py^{3,5}), 6.96 (s, 2H, mes), 6.44 (s, 2H, mes), 4.23 (m, 1H, OCH₂(CH₂)₂CH₃), 4.11 (m, 1H, OCH₂(CH₂)₂CH₃), 4.08 (s, 3H, OCH₃), 3.96 (bs, 4H, Im), 2.66 (s, 6H, CH₃^{mes}), 2.13 (s, 6H, CH₃^{mes}), 1.88 (m, 2H, OCH₂CH₂CH₂CH₃), 1.64 (s, 6H, CH₃^{mes}), 1.53 (m, 2H, O(CH₂)₂CH₂CH₃), 0.99 (t, 3H, $^3J_{\text{HH}} = 7.3$ Hz, O(CH₂)₃-CH₃) ppm.

X-ray structure determination

X-ray data of **4a**-CH₂Cl₂ were collected on a Bruker Kappa 8 APEX-2 CCD diffractometer using graphite-monochromated Mo-K α radiation ($\lambda = 0.71073$ Å) and 0.5° φ - and ω -scan frames. Corrections for absorption and $\lambda/2$ effects were applied [32]. After structure solution with program SHELXS97 and direct methods, refinement on F^2 was carried out with program SHELXL97 [33]. All non-hydrogen atoms were refined anisotropically. H atoms were placed in calculated positions and thereafter treated as riding. Crystallographic data are: **4**-CH₂Cl₂, C₃₂H₃₉Cl₂N₃-ORu-CH₂Cl₂, $M_r = 817.61$, green prism, 0.35 × 0.26 × 0.13 mm, triclinic, space group $P-1$ (no. 2), $a = 8.0798(4)$ Å, $b = 14.5694(6)$ Å, $c = 16.5689(7)$ Å, $\alpha = 72.937(2)^\circ$, $\beta = 81.987(2)^\circ$, $\gamma = 86.486(2)^\circ$, $V = 1845.97(14)$ Å³, $Z = 2$, $\mu = 0.753$ mm⁻¹, $d_x = 1.471$ g cm⁻³, $T = 100$ K. 65819 reflections collected ($\theta_{\text{max}} = 26.0^\circ$) and merged to 7228 independent data ($R_{\text{int}} = 0.0274$); final R indices (all data): $R_1 = 0.0218$, $wR_2 = 0.0541$, 440 parameters. CCDC 1054954 contains the supplementary crystallographic data for this paper. These data can be obtained free of charge from The Cambridge Crystallographic Data Centre via http://www.ccdc.cam.ac.uk/data_request/cif.

Testing of the solubility

After dissolving 1 mg of the respective compound in 5 cm³ CH₂Cl₂, removal of the solvent under N₂ stream, stirring, and drying of the residue, exactly 1 cm³ of the solvent to be tested was added. Upon stirring for 20 min at 25 °C, the samples were investigated by optical inspection. Transparent colored solutions without any residual solids were taken as indication of a solubility of 0.001 mol dm⁻³ (i.e., 1 mg cm⁻³) or better. The coexistence of solids and a colored solution was assigned to a solubility range of <1 and >0.1 mg cm⁻³. The appearance of uncolored solvents along with solid residues was interpreted as negligible solubility of the complexes in these solvents (<0.1 mg cm⁻³).

ROMP experiments

Monomer **6** (0.48 mmol, 300 equiv.) was dissolved in the respective solvent (CH₂Cl₂ or toluene, under exclusion of air) to obtain a solution with $c = 0.1$ mol dm⁻³, which was heated to the desired reaction temperature (40 or 80 °C oil bath temperature). The respective initiator (**4a–4d** or **5**, 0.0015 mmol, 1 equiv.) was added using a stock solution (4 mg cm⁻³) in the according solvent. The polymerization was monitored via thin layer chromatography and quenched upon addition of excess ethyl vinyl ether (approx. 0.1 cm³) after the spot for the monomer was not detected anymore. The volume of the reaction mixture was reduced to approx. 1.5 cm³. The polymer was obtained upon precipitation in vigorously stirred methanol and drying in vacuo. NMR spectroscopic data of the polymers are identical to those published previously [34, 35]. Polymerizations of monomers **6** and **8** in NMR tubes were carried out at 20 °C similarly using either CDCl₃ or methanol-*d*₄ as the solvents. Monomer **6** (10 equiv.; $c = 0.06$ mol dm⁻³) was polymerized with initiators **4a–4d** and **5** (1 equiv.). Monomer **8** (70 equiv.; $c = 0.13$ mol dm⁻³) was polymerized with **4b** (1 equiv.).

Simultaneous thermal analysis

A stock solution of the respective initiator in CH₂Cl₂ was prepared so that the desired initiator amount (40 ppm) is reached upon adding 0.06 cm³ of the solution to 1 cm³ of molten DCPD at approx. 35 °C. Both liquids were mixed and a weighed portion of the formulation was transferred to an open crucible which was placed in the STA-machine. A heating run (heating ramp of 3 °C min⁻¹) was commenced starting at 20 °C.

Acknowledgments Financial support by the European Community (grant no. CP-FP 211468-2 EUMET) is gratefully acknowledged. E.P. is thankful for having received the “Chemical Monthly” stipend 2013.

References

1. Grubbs RH (2003) Handbook of Olefin Metathesis. Wiley-VCH, Weinheim
2. Grela K (2014) Olefin metathesis, theory and practice. Wiley, Hoboken
3. Pump E, Cavallo L, Slugovc C (2015) Monatsh Chem. doi:10.1007/s00706-015-1433-8
4. Diesendruck CE, Tzur E, Ben-Asuly A, Goldberg I, Straub BF, Lemcoff NG (2009) Inorg Chem 48:10819
5. Benitez D, Tkatchouk E, Goddard WA III (2008) Chem Commun 46:6194
6. Credendino R, Poater A, Ragone F, Cavallo L (2011) Catal Sci Technol 1:1287

7. Prühs S, Lehmann CW, Fürstner A (2004) *Organometallics* 23:280
8. Slugovc C, Perner B, Stelzer F, Mereiter K (2004) *Organometallics* 23:3622
9. Leitgeb A, Mereiter K, Slugovc C (2012) *Monatsh Chem* 143:901
10. Stewart IC, Benitez D, O'Leary DJ, Tkatchouk E, Day MW, Goddard WA III, Grubbs RH (2009) *J Am Chem Soc* 131:1931
11. Ginzburg Y, Anaby A, Vidavsky Y, Diesendruck CE, Ben-Asuly A, Goldberg I, Lemcoff NG (2011) *Organometallics* 30:3430
12. Ung T, Hejl A, Grubbs RH, Schrodi Y (2004) *Organometallics* 23:5399
13. Gstrein X, Burtscher D, Szadkowska A, Barbasiewicz M, Stelzer F, Grela K, Slugovc C (2007) *J Polym Sci Part A Polym Chem* 45:3494
14. Abbas M, Slugovc C (2011) *Tetrahedron Lett* 52:2560
15. Abbas M, Slugovc C (2012) *Monatsh Chem* 143:669
16. Songis O, Slawin AMZ, Cazin CSJ (2012) *Chem Commun* 48:1266
17. Bantreil X, Poater A, Urbina-Blanco CA, Bidal YD, Falivene L, Randall RAM, Cavallo L, Slawin AMZ, Cazin CSJ (2012) *Organometallics* 31:7415
18. Urbina-Blanco CA, Bantreil X, Wappel J, Schmid TE, Slawin AMZ, Slugovc C, Cazin CSJ (2013) *Organometallics* 32:6240
19. Pump E, Poater A, Zirngast M, Torvisco A, Fischer R, Cavallo L, Slugovc C (2014) *Organometallics* 33:2806
20. Chandrasekhar S, Reddy NR, Rao SY (2006) *Tetrahedron* 62:12098
21. Slugovc C, Perner B, Stelzer F, Mereiter K (2010) *Acta Cryst E* 66:m154
22. Broggi J, Urbina-Blanco CA, Clavier H, Leitgeb A, Slugovc C, Slawin AMZ, Nolan SP (2010) *Chem Eur J* 16:9215
23. Burtscher D, Lexer C, Mereiter K, Winde R, Karch R, Slugovc C (2008) *J Polym Sci Part A Polym Chem* 46:4630
24. Leitgeb A, Wappel J, Urbina-Blanco CA, Strasser S, Wappl C, Cazin CSJ, Slugovc C (2014) *Monatsh Chem* 145:1513
25. Jeong W, Kessler MR (2008) *Chem Mater* 20:7060
26. Zirngast M, Pump E, Leitgeb A, Albering JH, Slugovc C (2011) *Chem Commun* 47:2261
27. Pump E, Fischer RC, Slugovc C (2012) *Organometallics* 31:6972
28. Bauer T, Slugovc C (2010) *J Polym Sci A Polym Chem* 48:2098
29. Falivene L, Poater A, Cazin CSJ, Slugovc C, Cavallo L (2013) *Dalton Trans* 42:7312
30. Matsuo T, Yoshida T, Fujii A, Kawahara K, Hirota S (2013) *Organometallics* 32:5313
31. Kirmse W, Mrotzek U, Siegfried R (1991) *Chem Ber* 124:241
32. Bruker programs: APEX2, version 2009.9-0; SAINT, version 7.68 A; SADABS, version 2008/1; SHELXTL, version 2008/4, Bruker AXS Inc., Madison
33. Sheldrick GM (2008) *Acta Crystallogr A* 64:112
34. Riegler S, Demel S, Trimmel G, Slugovc C, Stelzer F (2006) *J Mol Catal A* 257:53
35. Slugovc C, Demel S, Riegler S, Hobisch J, Stelzer F (2004) *J Mol Catal A* 213:107